Available online at www.sciencedirect.com

ScienceDirect

Procedia Engineering 64 (2013) 1474 – 1484

Procedia Engineering

www.elsevier.com/locate/procedia

International Conference On DESIGN AND MANUFACTURING, IConDM 2013

Heat Transfer Enhancement with Al_2O_3 Nanofluids and Twisted Tapes in a Pipe for Solar Thermal Applications

Y. Raja Sekhar[a,]*, K.V.Sharma[b], R.Thundil Karupparaj[a], C.Chiranjeevi[a]

[a] *School of Mechanical and Building Sciences, VIT University, Vellore, Tamilnadu- 632014, India*
[b] *JNTUH College of Engineering, Manthani, Andhra Pradesh- 515025, India*

Abstract

Solar thermal energy is currently used for low temperature heating applications using flat plate collectors. The absorbed solar energy is transferred to the working fluid flowing in the pipe. The performance of the system is influenced by heat transfer from tube to working fluid, with minimum convective losses, which has to be considered as one of the primary design factor. In tube and channel flows, to enhance the rate of heat transfer to the working fluid, passive augmentation techniques such as twisted tapes and swirl generators are used in the fluid flow path. In this paper, convective heat transfer analysis for a horizontal circular pipe with fluid in mixed laminar flow range is performed using experimental simulation under constant heat flux boundary condition. The variation of heat transfer coefficient and pressure drop in the pipe flow for water and water based Al_2O_3 nanofluids at different volume concentrations and twisted tapes are studied. The dependence of particle concentration and Reynolds number for enhancement in heat transfer and increase in the pumping power due to pressure drop is analysed in the range of parameters considered.

Selection and peer-review under responsibility of the organizing and review committee of IConDM 2013

Keywords: Laminar Convective heat transfer; friction factor; twisted tapes; Al_2O_3 nanofluids; Constant wall heat flux; Local Nusselt number

1. Introduction

In many engineering applications having heating or cooling process, solar energy is widely used. For most of the domestic water heating purposes, solar flat plate collectors are employed. The heat exchange phenomenon between

* Corresponding author. Tel.: +91-9962155819; fax: +91-416-2243092.
E-mail address: rajasekhar.y@vit.ac.in

1877-7058 © 2013 The Authors. Published by Elsevier Ltd.
Selection and peer-review under responsibility of the organizing and review committee of IConDM 2013
doi:10.1016/j.proeng.2013.09.229

the fluid and surrounding high temperature source is governed by convective heat transfer. In the current era, high performance heat transfer equipment with minimal surface area is the industrial requirement. Also, to derive optimal energy conversion, the design of the system must provide high efficiency at low cost. Usually in all solar energy applications, the efficiency is governed by the collector area and amount of incident solar radiation. The enhancement of heat dissipation to the working fluid and using a working fluid of high heat transfer performance will increase the efficiency of collectors. For more than a decade, researchers had performed many studies in the past to show enhanced properties of nanofluids [1-3] and will result a certain increase in the heat transfer characteristics in tube flow [4-8]. But, heat convection characteristics in practical heat exchange mechanisms must also be studied [9]. Many researchers have focused experimental and numerical investigations for forced convection heat transfer studies in a pipe with different material and concentration of nanoparticles, inserts and boundary conditions in turbulent and laminar flow regime in plain tubes [10-16]. Yung et al. [17] studied the convective heat transfer coefficient and friction factor in rectangular micro channels using Al_2O_3 – water/ethylene glycol (50:50) nanofluid with different concentrations. Their results had shown increase in

Nomenclature

c_p	Specific heat of the fluid, kJ/kg-K
d_p	diameter of the particle, nm
D	diameter of tube, mts
f	Friction factor
h	Heat transfer coefficient, W/ m^2-K
I	Current, amps
K	Thermal conductivity, W/m^2
L	length of the tube
m	mass flow rate, kg/s
Nu	Nusselt number
Pr	Prandtl number
q	heat input, watts
q”	heat flux, W/m^2
Re	Reynolds number
T	Temperature of fluid, ^{0}C
V	Voltage, Volts
x	axial distance from the entrance region of tube, mts
Greek symbols	
ρ	Density, kg/m^3
ϕ	Volume concentration, %
μ	Dynamic viscosity, kg/m-s
δ	Boundary layer thickness
α	Thermal diffusivity, m^2/s
Sub-scripts	
f	fluid
in	inlet
m	bulk mean
nf	nanofluid
out	outlet
p	particle
s	surface
Reg	Regression

convective heat transfer with increase in Reynolds number of flow and enhanced by 32% at 1.8% volume concentration. Kolade et al. [18] studied convective heat transfer performance in laminar thermally developing flow with Al_2O_3 – water and Silicone oil/MWCNT nanofluids. They observed that augmentation factor for water - Al_2O_3 nanofluid is very less compared to silicone oil with MWCNT. Wen and Ding [6] conducted experimental investigations under laminar flow conditions at the entrance region of the tube using water and γ-Al_2O_3 nanoparticles. They proposed that the reason for enhancement might be migration of particles and the resulting disturbance of the boundary layer. The rate of heat transfer depends on the thermal and hydraulic properties in the system. Usually, to enhance the heat transfer rate in pipe flows, twisted tapes are employed which provides many advantages in heat exchanger applications. It becomes significant where, there is no additional heat transfer area is required. It is usually mistaken that, use of twisted tape inserts lead to increased tube side pressure drop. But, in comparison to plain tube it can always be shown that tube with inserts have heat transfer enhancement at the same or even lower pressure drop [15]. Due to insertion of twisted tapes in the flow path, greater flow length is induced and generates swirl which affects the transverse fluid transport across the tape-partitioned pipe section, there by promoting greater fluid mixing and high heat transfer rates [15]. Sharma et al. [16,19] have investigated convective heat transfer of Al_2O_3 nanofluids in plain tube with twisted tape insert under turbulent flow conditions. Their results indicated enhancement of Nusselt number compared to the plain tube at the same flow conditions. Also, a few researchers have attempted convective heat transfer studies for solar collector applications using twisted tapes in turbulent flow regime [20]. From the literature study it is understood that using nanofluids will increase the convective heat transfer, but will also increase the pumping power. This study is intended to estimate the heat transfer coefficients for forced convection and uniform heat flux boundary condition in the laminar flow range. Aqueous Al_2O_3 nanofluids of various concentrations and twisted tapes under different uniform axial heat flux condition are tested. The estimated heat transfer coefficients are compared with the data available in Literature.

2. Experimental setup and procedure

An Experimental test setup was fabricated to investigate the convective heat transfer and friction factor behaviour of water based Al_2O_3 nanofluids in a horizontal circular tube subjected to constant heat flux boundary condition. The schematic diagram of the experimental setup and twisted tape is shown in Figure 1a and 1b respectively. The fluid is allowed to flow through a copper tube of 0.012 m diameter resembling the riser tube of solar flat plate collector. The flow circuit consists of a chiller, collecting tank, and a storage tank connected to a pump. The copper tube is heated uniformly by wrapping it with two nichrome heaters of 20 gauge, having a resistance of 53.5 ohms per meter length and 1000 W maximum rating, and the entire test section is subject to a constant heat flux boundary condition. The space between the test section and the outer casing is insulated with rock wool to minimize heat loss. The test section of 1.5 m in length is provided with five K-type thermocouples in which three were brazed to the surface at distances of 0.375, 0.75, 1.125 m from entry and two located to measure the working fluid inlet and outlet temperatures. All these thermocouples have 0.1^0C resolution and are calibrated before fixing them at the specified locations and the accuracy is within 0.4^0C. Experiments are conducted with distilled water with a view to test the accuracy of the results. The aspect ratio of the test section is sufficiently large for the flow to be hydro-dynamically developed. The fluid from the storage tank is forced through the test section with the aid of a pump connected to the suction side of the tank. The liquid is heated in the test section and hot fluid is allowed to cool by passing it through a chiller. The provision of the chiller helps to achieve the steady inlet fluid temperature. The procedure for preparation of nanofluids follows Syam Sundar et al. [3]. Nanofluid at different volume concentrations of 0.02, 0.1 and 0.5% is used in conducting the experiments. The thermal and properties of nanofluids such as thermal conductivity, density, viscosity and specific heat of the nanofluids at different concentrations are estimated using the equations (1) – (4) respectively based on the previous work of Sharma et al. [16].

$$K_r = \frac{K_{nf}}{K_f} = 0.8938\left(1+\frac{T_{nf}}{70}\right)^{0.2777}\left(1+\frac{d_p}{150}\right)^{-0.0336}\left(1+\frac{\phi}{100}\right)^{1.37}\left(\frac{\alpha_p}{\alpha_w}\right)^{0.01737} \quad (1)$$

$$\rho_{nf} = \phi\rho_p + (1-\phi)\rho_w \quad (2)$$

$$\mu_{nf} = \mu_w \left(\left(1 + \phi/100 \right)^{11.3} \left(1 + \frac{T_{nf}}{70} \right)^{-0.038} \left(1 + \frac{d_p}{170} \right)^{-0.061} \right) \quad (3)$$

$$C_{p_{nf}} = C_p + (1-\phi) C_{p_w} \quad (4)$$

The flow rates are calculated by collecting the fluid in a collecting vessel over a period of time with the help of a precise measuring jar and stop watch. At the ends of the test section 3mm hole is drilled with the help of drilling machine to tap the pressure across the test section. One end of the manometer is connected with the inlet tap, and the other end of the monometer is connected with the outlet tap. The readings of the level in the U-tube are noted down and made equal. Due to the working fluid pressure, the fluid level in the U-tube changes and the difference in height of the levels are measured. The fluid line connections are checked for leaks after filling the storage tank with the working fluid (water & nanofluids). The Reynolds number of flow of the working fluid flowing in the test section is measured from the mass flow rate. The total heat transfer test section is heated with constant heat flux boundary condition. All the heat transfer tests and friction factor tests are conducted in the flow Reynolds number form 800 - 2200. Total 80 data points are generated for the estimation of heat transfer coefficient and friction factor with twisted tape inserts. Regression equations are developed for the estimation of Nusselt number and friction factor for fluid flowing in a tube with and without tape inserts based on the experimental data.

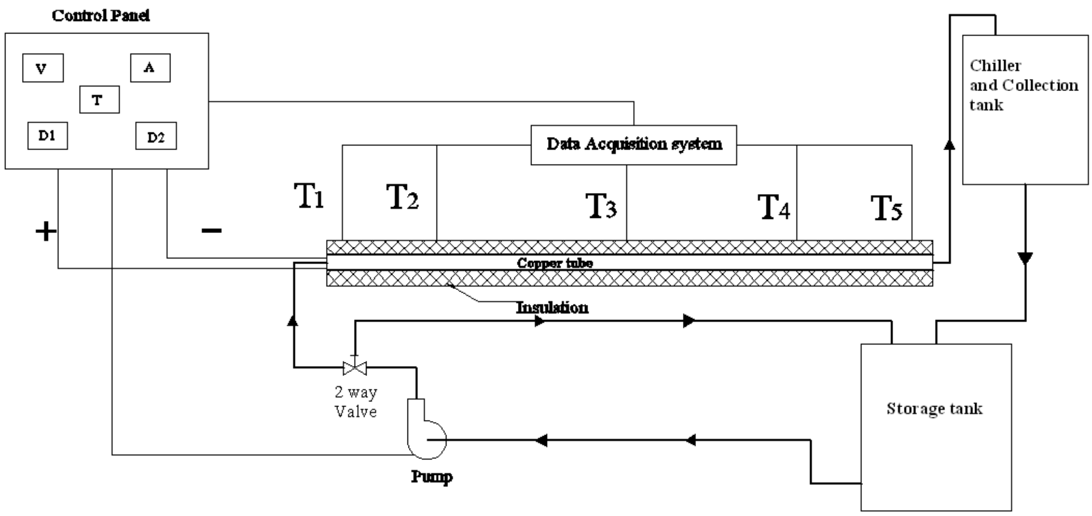

Fig. 1. (a) Schematic diagram of the experimental system

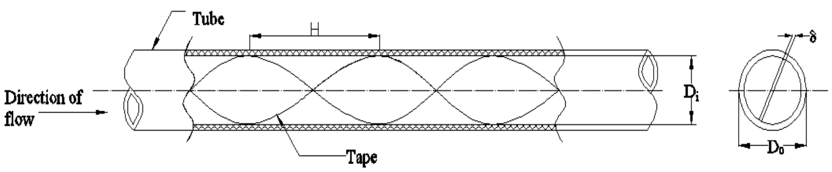

Fig. 1 (b) Full length twisted tape insert inside a tube

3. Data Analysis

In the experiments conducted under constant heat flux boundary condition, temperature of pipe surface at different locations, Voltage and current supplied to the heater and pressure drop is recorded. The heat transfer coefficient is estimated with Newton's law of cooling. The energy balance between the heat supplied and energy absorbed by the flowing liquid is established using Eqns. (5) and (6) for every set of data and the experimental heat transfer coefficient is estimated with Eqn. (7).

$$q = V \times I \quad (5) \qquad q = \left(\dot{m} C_p (T_{out} - T_{in})\right) \quad (6) \qquad h = \frac{q''}{(T_s - T_m)} \quad (7)$$

The deviation between the values obtained with Eqns. (5) and (6) is less than ± 2.5% and the heat loss to atmosphere is neglected. The net heat input to the test section is corrected for electrical heat input to the fluid by calculating the losses through the insulation. The experiments were performed for each run after ensuring the difference between the net heat input and enthalpy rise of the fluid is less than 5%. The enthalpy rise of the fluid is calculated from equation 6.

The bulk temperature of the fluid at any axial position of the tube at a distance of x from the inlet is calculated by assuming linear temperature variation along the length. The local heat transfer performance was defined in terms of the Nusselt number (Nu_x) and heat transfer coefficient (h_x) is given by

$$Nu_x = \frac{h_x D}{k} \quad (8) \qquad h_x = \frac{q''}{\left(T_{i,W}(x) - T_{m,f}(x)\right)} \quad (9)$$

Where h_x is the local heat transfer coefficient

Since, the inner wall temperature of the tube could not be measured directly, it can be determined from the heat conduction equation in the cylindrical coordinate system given by equation (10) [1].

$$T_{i,W}(x) = T_{o,W}(x) - \frac{q\left[2D_o^2 \ln\left(\frac{D_o}{D_i}\right) - \left(D_o^2 - D_i^2\right)\right]}{4\pi\left(D_o^2 - D_i^2\right)K_s x} \qquad (10)$$

The mean temperature of the fluid $T_{m,f}(x)$ at any axial position from the entrance can be determined from the energy balance equation at that section of the tube for the constant heat flux boundary condition. From the first law of control volume of the length, dx of the tube with incompressible fluid and negligible pressure, the convective heat transfer is given by equation (11).

$$dq_{conv} = q'' p.dx = \dot{m} C_p dT_m \quad (11)$$

Where p is the perimeter of the test section given by πD_i and dT_m is the differential mean temperature of the fluid in that section.

Therefore, $$dT_m = \frac{q'' \pi D_i}{\dot{m} C_p} dx \qquad (12)$$

The variation of T_m with respect to axial distance x can be determined by integrating the above equation from $x = 0$ to x and mean temperature of the fluid is given by

$$T_{m,f}(x) = T_{in} + \frac{(T_{out} - T_{in})}{L} x \quad (13)$$

Therefore, *(14)*

$$h_x = \frac{q''}{\left(\left\{T_{o,W}(x) - \frac{q\left[2D_o^2 \ln\left(\frac{D_o}{D_i}\right) - \left(D_o^2 - D_i^2\right)\right]}{4\pi\left(D_o^2 - D_i^2\right)K_s x}\right\} - \left[T_{in} + \frac{\left(T_{out} - T_{in}\right)}{L}x\right]\right)}$$

The Nusselt number can also be determined from the well-known Shah correlation for laminar flows under constant heat flux boundary condition given by [10,11]

$$\mathrm{Nu} = 1.963\left(\mathrm{Re.Pr.}\frac{\mathrm{D}}{\mathrm{x}}\right)^{1/3} \; for \; \left(\mathrm{Re.Pr.}\frac{\mathrm{D}}{\mathrm{x}}\right) \geq 33.3 \qquad (15)$$

The fluid in the test section having uniform cross sectional area is assumed to be incompressible and flow is steady. Reynolds number of flow is defined as

$\mathrm{Re} = \dfrac{4\dot{m}}{\pi D_i \mu_f}$ and Prandtl number is defined as $\mathrm{Pr} = \dfrac{C_p \mu_f}{K_f}$

Similarly, average heat transfer coefficient and Nusselt number of flow is calculated using

$$h = \frac{q''}{\left(\overline{T_w} - \overline{T_f}\right)} \quad \text{and} \quad Nu_m = \frac{hD}{K}$$

where, $\overline{T_w}$ is the average temperature of the wall and $\overline{T_f}$ is the mean bulk fluid temperature.

Similarly, the pressure drop across the test section was measured by U-tube manometer which is connected at the either ends of the test section as shown in the experimental setup Fig. 1(a). CCl_4 was used as the manometer fluid since the density of the fluid is higher than that of the working fluid. Before taking the pressure drop measurements, the test section was freed of air bubbles by venting them to the reservoir tank placed at the end of the test section. The Darcy friction factor is calculated from the measured pressure drop using equation (16).

$$f = \frac{\Delta P}{\left(\frac{\rho V^2}{2}\right)}\frac{D}{L} \qquad (16)$$

where $\Delta P = \rho g h$

But, for laminar flows friction factor is given by $f = \dfrac{64}{\mathrm{Re}}$ *(17)*

4. Results and discussion

To validate the experimental setup, measurements were first evaluated for Nusselt number and friction factor by conducting experiments in a plain tube with water at different Reynolds number. The experimental local Nusselt number data is compared with numerical results and experimental data from Literature [6,10,11] as shown in Fig 2. The variation of friction factor for water in a plain tube with increasing Reynolds number is shown in Fig 3. It is observed that equation of Shah [10,11] is under predicting the local Nusselt numbers by over 15%. A similar trend was observed by Wen and Ding [6] and Kim et al. [21] in their experimental results and the reason is presumably because of the tube size where the Shah equation was developed for large channels [6]. The deviation of present experimental values compared to experimental data of literature is found to be less than 10% hence validating the experimental setup. The variation of local Nusselt number along the dimensionless axial distance for different Reynolds number of water in a plain tube is shown in Fig 4. It can be observed that for increasing Reynolds number, the local Nusselt number is increasing by over 20% at the same axial position. Further, the variation of local Nusselt number in plain tube with use of nanofluids is experimentally studied. The data of local Nusselt number along the axial distance for different flow Reynolds number is shown in Fig 5. The Reynolds number will change with use of nanofluids due to small variations in viscosity at different particle concentrations. The changes in values of Reynolds number in Fig.5 are within ± 100. It can be observed that with use of nanofluids the heat transfer coefficient certainly enhances especially in the entrance region. The local heat transfer coefficient at X/D =10 and 0.5% particle concentration is 26% and 22% higher than compared to water in a plain tube. It is also observed that the local Nusselt number increases with Reynolds number and particle concentration. But, a significant decrease in heat transfer enhancement with increase axial distance is noted. A similar trend was observed by Wen and Ding [6] in their experimental results using Al_2O_3 nanofluids up to 1.6% volume concentration.

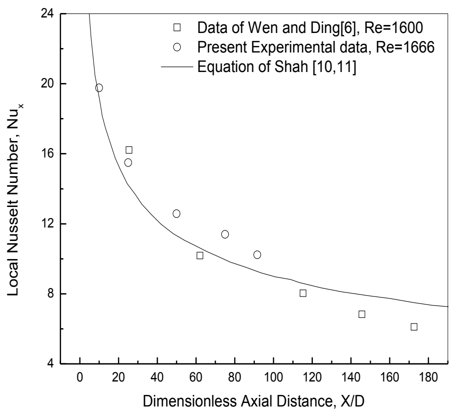

Fig 2. Comparison of Local Nusselt number of plain tube

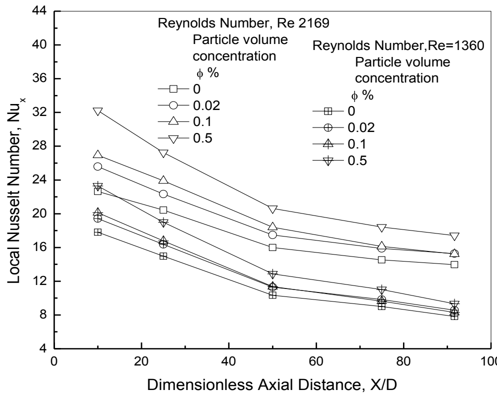

Fig 4. Variation of Local Nusselt number along the dimensionless axial distance for water in plain tube at different flow Reynolds number

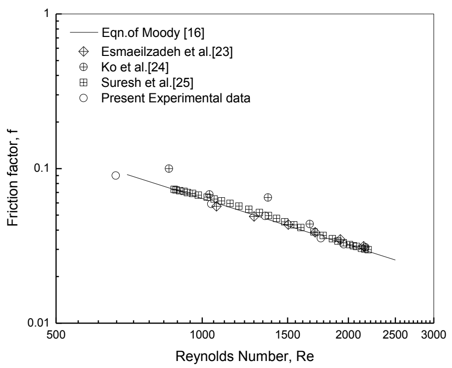

Fig 3. Comparsion of friction factor for water in plain tube at different flow Reynolds number using water with data of literature

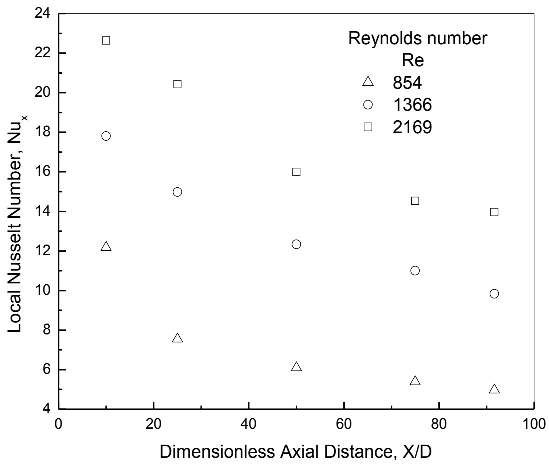

Fig 5. Variation of Local Nusselt number along the dimensionless axial distance for water and nanofluids in plain tube at different flow Reynolds number

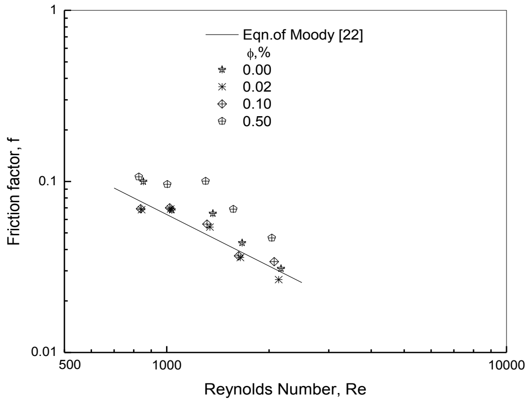

Fig 6. Variation of friction factor for water and nanofluids in plain tube at different flow Reynolds number

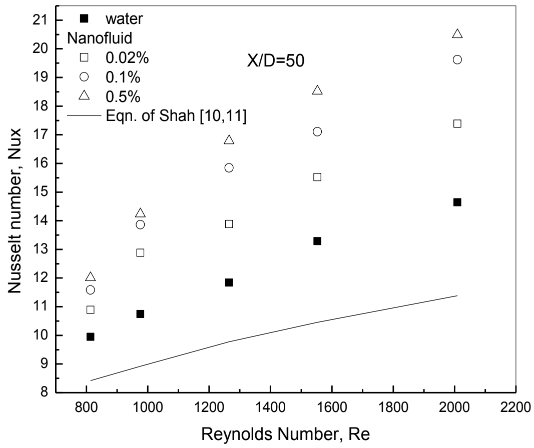

Fig 7. Variation of local Nusselt number for different volume fractions of nanofluids at X/D=50 for tube with H/D=5

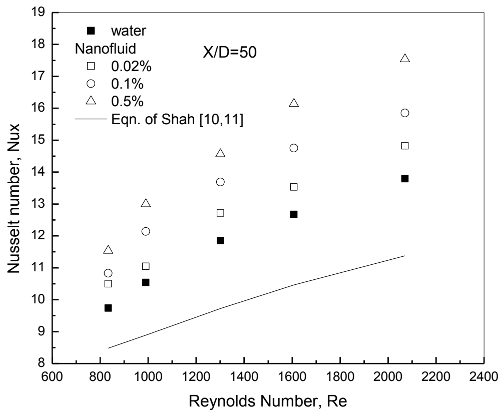

Fig 8. Variation of local Nusselt number for different volume fractions of nanofluids at X/D=50 for tube with H/D=10

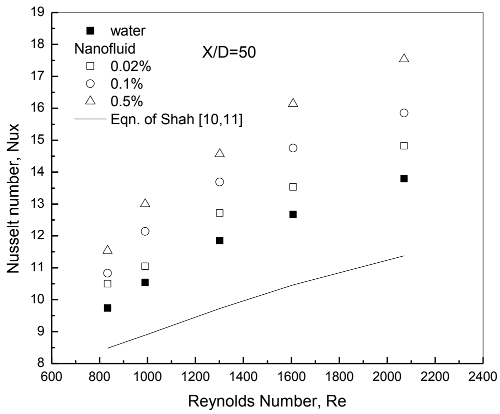

Fig 9. Variation of local Nusselt number for different volume fractions of nanofluids at X/D=50 for tube with H/D=15

Friction factor measured from the experiments for plain tube with water is presented in Fig. 6 and compared with equation of Moody [22]. The deviation of present experimental friction factor for water to the equation of Moody is found to be less than 5%. It can be observed that for increasing particle concentration the friction factor is increasing while for increasing Reynolds number the friction factor decreases. The variation of friction factor for different nanofluids is presented in Fig 4(a). Regression equations are developed for average Nusselt number and friction factor in a plain tube using water and nanofluids given by equations (5) and (6) valid in the range $0< \phi <$ 0.5%. The deviation of estimated values from measured values of average Nusselt number and friction factor using regression equations are less than 10% as shown in Figs. 5 and 4(b) respectively. The friction factor for different volume concentrations of Nanofluid calculated from the eqn. (6) are compared with the values of plain water and observed that the friction values of nanofluid are slightly higher than the values of water due to increase in fluid viscosity and decrease in Reynolds number. The Nusselt number increase for nanofluids compared to plain water is of the order of 8-12% for all the particle volume concentrations. The possible reasons for the enhancement of Local heat transfer coefficient are discussed here under.

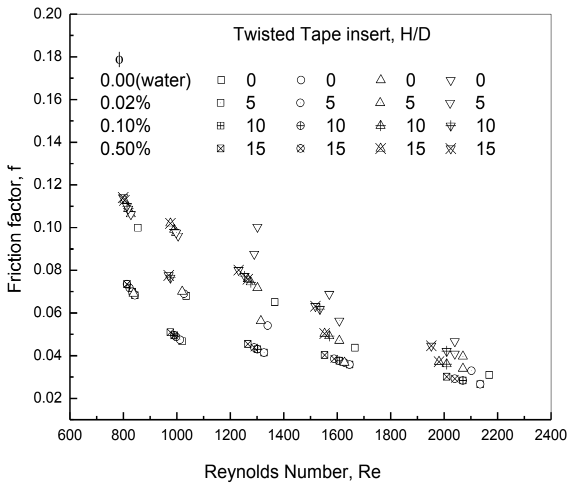

Fig 10. Variation of friction factor for different volume fractions of nanofluids and twist ratio

For a flow having uniform velocity and temperature distributions through the pipe, the fluid has different temperature from the wall temperature. Experimental Local heat transfer coefficient for different volume concentrations of nanofluid with twisted tape inserts is shown in the Figs. 5 – 8. From the figures it can clearly observed that the nanofluid of 0.5% volume concentration with twisted tape of H/D = 5 is having high heat transfer coefficients compared to the other data. Twisted tapes insertion and consideration of nanofluids for heat transfer enhancement result in increase of pressure drop in the flow, which contribute to increase of pumping power. Pumping power increase is calculated on the basis of Fanning frictional factor. The ratio of increase of Fanning frictional loss due to increase in density and viscosity of nanofluids to the Fanning friction loss due to water will give the increase in pumping power required. The reason for heat transfer enhancement of nanofluid with twisted tape insert is the effect of Prandtl number. The similar trend was observed by Sarma et al. [26] for single phase fluid with twisted tape inserts. How ever for comparison of experimental data with nanofluid and twisted tape inserts under laminar flow conditions, data is not available in the literature.

5. Conclusions

Heat transfer experiments were conducted in a pipe under low Reynolds number range using water and water based nanofluids. Heat transfer coefficient and friction factor for nanofluid in the flow path enhanced compared to water. The experimental data is compared with the data of literature and are found to be in good agreement. The increase in heat transfer coefficient in plain tube with use of nanofluids is greater by 8-12% compared to the flow of water in a plain tube. The nanofluid of 0.5% particle concentration is having highest friction factor compared to water. The Nusselt number and friction factor increases with increase of particle concentration. But, friction factor decreases with increase of Reynolds number of flow where as the Nusselt number increases. Using nanofluid with a high heat exchange can help in reduce the size of the heat exchanger or with out increasing the size of the heat exchanger efficiency of the system can be improved. Further, using twisted tapes and nanofluids in the pipe flows is advantageous since it is visible from the results that the energy gained with heat exchange is more than the energy spent on pumping power. It is clear from the results that heat transfer enhancement in a horizontal tube increases with Reynolds number of flow and nanoparticle concentration.

Acknowledgements

The author is thankful to the technical staff of the Thermo Fluids Laboratory for their support in the conduct of the experiment. The financial support by the Centre for Energy Studies, JNTUH College of Engineering, Kukatpally, Hyderabad is gratefully acknowledged.

References

[1] Choi, S.U.S, Enhancing thermal conductivity of fluids with nanoparticles developments and applications of Non-Newtonian flows, FED-Vol.231/MD.66, 1195, p.99-105.

[2] Raja Sekhar, Y., Sharma, K.V., Naik, M.T., Syam Sundar, L., 2012. Experimental investigations on thermal conductivity of water and Al_2O_3 nanofluids at low concentrations, International Journal of Nanoparticles, No.4, 5, p. 300-315(16).

[3] Syam Sundar, L., Sharma, K.V., 2008. Thermal conductivity enhancement of nanoparticles in distilled water, International Journal of Nanoparticles, Vol. 1, No. 1, p. 66-77.

[4] Pak, B.C., Cho, Y., 1998. Hydrodynamic and heat transfer study of dispersed fluids with submicron metallic oxide particle, Exp. Heat Transfer 11, p. 151–170.

[5] Xuan, Y., Li, Q., 2003. Investigation on convective heat transfer and flow features of nanofluids, ASME J. Heat Transfer 125, p. 151–155.

[6] Wen, D., Ding, Y., 2004. Experimental investigation into convective heat transfer of nanofluid at the entrance region under laminar flow conditions, Int. J. Heat Mass Transfer 47, p. 5181–5188.

[7] Ding, Y., Alias, H., Wen, D., Williams, R.A., 2006. Heat transfer of aqueous suspensions of carbon nanotubes (CNT nanofluids), Int. J. Heat Mass Transfer 49, p. 240–250.

[8] Buongiorno, J., 2006. Convective transport in nanofluids, ASME J. Heat Transfer 128, p. 240–250.

[9] Tun-Ping Teng, Yi-Hsuan Hung, Tun-Chien Teng, and Jyun-Hong Chen, 2011. Performance evaluation on an air-cooled heat exchanger for alumina nanofluid under laminar flow, Nanoscale Res Lett. 6(1), p. 488.

[10] Shah, R.K., London, A.L., 1978. Laminar flow forced convection in ducts, Supplement to Advances in Heat Transfer, Academic Press, New York.

[11] Shah, R.K., Bhatti, M.S., 1987. Laminar convective heat transfer in ducts, in: S. Kakac, R.K. Shah, W. Aung (Eds.), Handbook of Single-Phase Convective Heat Transfer, Wiley, New York, (Chapter 3).

[12] Xuan, Y., Roetzel, W., 2000. Conceptions for heat transfer correlation of nanofluids, Int. J. Heat Mass Transfer 43, p. 3701–3707.

[13] Kyo Sik Hwang , Seok Pil Jang , Stephen U.S. Choi, 2009. Flow and convective heat transfer characteristics of water-based Al_2O_3 nanofluids in fully developed laminar flow regime, International Journal of Heat and Mass Transfer 52, p. 193–199.

[14] Shon, C.W., Chen, M.M., 1981. Microconvective thermal conductivity in disperse two-phase mixture as observed in a low velocity Couette flow experiment, ASME J. Heat Transfer 103, p. 47–51.

[15] Mazen M.Abu-Khader, 2006. Further understanding of twisted tape effects as tube insert for heat transfer enhancement, Heat and Mass transfer 43, p. 123-134.

[16] Sharma, K.V., Sarma, P. K., Azmi, W. H., Rizalman Mamat and Kadirgama K., 2012. Correlations to Predict Friction and Forced Convection Heat Transfer Coefficients of Water Based Nanofluids For Turbulent Flow in a Tube, IJMNTFTP, Volume 3, Number 4 p. 1-25.

[17] Ying Yang, George Zhang, Z., Eric Grulke, A., William Anderson, B., Gefei Wu, 2005. Heat Transfer properties of nanoparticle-in-fluid dispersions (nanofluids) in laminar flow, International Journal of Heat and Mass Transfer 48, p. 1107-1116.

[18] Babajide Kolade, Kenneth Goodson, E., John Eaton, K., 2009. Convective Performance of Nanofluids in a Laminar Thermally Developing Tube Flow,Journal of Heat Transfer 131, p.052402-(1-8).

[19] Sharma, K.V., Syam Sundar, L., Sarma, P.K., 2009. Estimation of heat transfer coefficient and friction factor in the transition flow with low volume concentration of Al_2O_3 nanofluid flowing in a circular tube and with twisted tape insert, International Communications in Heat and Mass Transfer 36, p. 503–507.

[20] Kumar, A., Prasad, B.N., 2000. Investigation of twisted tape inserted solar water heaters - heat transfer, friction factor and thermal performance results, Renewable Energy 19, p. 379 – 398.

[21] Doohyun Kim, Younghwan Kwon, Yonghyeon Cho, Chengguo Li, Seongir Cheong, Yujin Hwang, Jaekeun Lee, Daeseung Hong, Seongyong Moon, 2009. Convective heat transfer characteristics of nanofluids under laminar and turbulent flow conditions, Current Applied Physics 9, p. 119–123.

[22] Sieder, E.N., Tate, C.E., 1936. Heat transfer and pressure drop of liquids in tubes, Ind. Eng. Chem. 28, p. 1429–1435.

[23] Moody, L., 1944. Friction Factors for Pipe Flow, Transactions of the ASME 66, 8, p. 671-684.

[24] Esmaeilzadeh, E., Almohammadi, H., Nasiri Vatan, Sh., Omrani, A.N., 2013. Experimental investigation of hydrodynamics and heat transfer characteristics of γ-Al_2O_3/water under laminar flow inside a horizontal tube, International Journal of Thermal Sciences 63, p. 31-37.

[25] Gwon Hyun Ko, Kyoungyoon Heo, Kyoungjun Lee, Dae Seong Kim, Chongyoup Kim, Yangsoo Sohn, Mansoo Choi, 2007. An experimental study on the pressure drop of nanofluids containing carbon nanotubes in a horizontal tube, International Journal of Heat and Mass Transfer 50, p. 4749–4753.

[26] Suresh, S., Chandrasekar, M., Chandra Sekhar, S., 2011. Experimental studies on heat transfer and friction factor characteristics of CuO/water nanofluid under turbulent flow in a helically dimpled tube, Experimental Thermal and Fluid Science 35, p. 542–549.

[27] Sarma, P.K., Subramanyam, T., Kishore, P.S., Dharma Rao, V., Sadik Kakac, 2002. A new method to predict convective heat transfer in a tube with twisted tape inserts for turbulent flow, International Journal of Thermal Sciences 41, p.955–960.